Progress In Electromagnetics Research C, Vol. 83, 125–136, 2018

Algebraic Algorithm for Mixed Near-Field and Far-Field Sources Classification and Localization

Kai Wang*, Ling Wang, Zhaolin Zhang, and Jian Xie

Abstract—Using uniform linear array (ULA), a passive localization algorithm is presented for mixed far-field (FF) and near-field (NF) signals scenarios. Based on the high-order cumulant (HOC) technique, a special Hermite matrix is constructed by three fourth-order cumulant matrices, which are calculated by dividing the ULA into two sub-arrays. Then, the special matrix of signals is decomposed to obtain the source subspace. According to ESPRIT algorithm, two transformation matrices of all sub-arrays can be obtained. Meanwhile, the two transformation matrixes could be used to calculate the range and angles of arrival (AOA) of NF sources, as well as AOAs of FF sources. Moreover, compared with two-stage MUSIC (TSMUSIC) and four-order cumulant MUSIC method, the proposed algorithm has higher accuracy for localisation of both FF and NF sources without any spectral search.

1. INTRODUCTION

Passive mixed source localisation using a sensor array has many important application areas such as radar and sonar [1, 2]. For far-field (FF) sources, only DOA parameters are needed to be estimated. However, for near-field (NF) sources, both the DOA and range parameters are required since the plane wave-front assumption is no longer valid. Although various algorithms focus on the pure FF or NF sources scenario [3–7], it is more realistic in many applications that FF and NF sources coexist, so that several typical solutions have been developed to solve this problem. In the mixed NF and FF sources scenario, the above mentioned algorithms may fail to distinguish and locate the mixed sources.

Recently, Liang and Liu [8] provided a four-order cumulant multiple signal classification (Cum4MUSIC) method to solve the mixed sources localization issue. This algorithm constructs a special HOC matrix to eliminate the range parameter in the steering vectors and estimates the DOAs of both FF and NF sources. With the estimated DOA estimates, the range parameters can be obtained by 1-D spectral search. It must be noticed that the steering vectors of NF sources can be approximated to high order polynomials by Taylor expansion. In the Fresnel Region, we often consider that higher than second order items of the polynomials are approximately equal to zero [9], i.e., the steering vectors of NF sources can be described as the quadratic function of the indexes of all sensors in the array which is uniformized by the half of free-space wavelength. However, the prior knowledge of which signals are NF or FF sources must be known. In [10], Liu and Sun used the spatial differencing technique to classify the NF sources from the mixed sources after the estimations of FF sources. The methods in [11, 12] are the promotion of the algorithms in [9, 10] from 2-D (AOA and range) to 3-D (azimuth angle, elevation angle and range). However, all aforementioned high-resolution methods depend on the spatial spectral search, which implies a very high computational cost.

In this paper, a mixed sources localization method is presented, which has low computational complexity. By dividing the ULA into two sub-arrays, the proposed method takes full advantage of the AOAs information of each source at different phase reference points to classify the sources rapidly,

Received 27 February 2018, Accepted 30 March 2018, Scheduled 12 April 2018
* Corresponding author: Kai Wang (wangk829@sina.com).
The authors are with the School of Electronic and Information, Northwestern Polytechnial University, China.

and localizes NF sources efficiently without any spectral search. Additionally, the proposed algorithm would avoid parameter matching and two-dimensional searching problems.

2. SIGNAL MODEL

Consider K (near-field or far-filed) narrowband and independent signal sources, impinging on a uniform array with $2L+1$ omnidirectional sensors. From left to right, the sensors are indexed by $-L$, $-(L-1)$, $\ldots$, $L-1$, L, and the centre of array is set to be the phase reference point whose index is zero. The signals received by the l-th sensor can be expressed as

$$z_l(t) = \sum_{k=1}^{K} s_k(t) e^{j\tau_{lk}} + n_l(t) \qquad l = -L, -L+1, \ldots, L-1, L \tag{1}$$

where $s_k(t)$ is the k-th narrowband source, $n_l(t)$ the additive Gaussian noise, and $\tau_{k,l}$ the phase shift associated with the k-th source propagation time delay between the phase reference point located at the 0-th and the l-th sensor. It is straightforward to show that the phase shift between the phase reference point and l-th sensor can be expressed as [13]

$$\tau_{k,l} = \frac{2\pi}{\lambda}\left(\sqrt{r_k^2 + (ld)^2 - 2r_k ld\sin\theta_k} - r_k\right) \tag{2}$$

where λ denotes the signal free-space wavelength. $\theta_k \in [-\pi/2, \pi/2]$ is the AOA of the k-th source; and $r_k \in [0.62(D^3/\lambda)^{1/2}, +\infty)$ stands for the range of the k-th source between the phase reference point; D represents the aperture of the array; d is the constant inter-element spacing, denoted as $d \leq \lambda/4$ [14, 15]. According to the Taylor expansion, $\tau_{k,l}$ can be approximately given as follows [16]

$$\begin{aligned} \tau_{k,l} &= \alpha_k l + \beta_k l^2 + O(l^3) \approx \alpha_k l + \beta_k l^2 \\ \alpha_k &= -2\pi\frac{d}{\lambda}\sin\theta_k \\ \beta_k &= \pi\frac{d^2}{\lambda r_k}\cos\theta_k \end{aligned} \tag{3}$$

Using the above approximation of $\tau_{k,l}$, the outputs of the l-th sensor can be described as

$$z_l(t) = \sum_{k=1}^{K} s_k(t) e^{j(\alpha_k l + \beta_k l^2)} + n_l(t) \tag{4}$$

Throughout the paper, the following hypotheses are assumed to hold:

1) The incoming source signals are statistically independent and zero-mean stationary random process with nonzero kurtosis;
2) The sensor noise is the additive (white or color) Gaussian one, which is independent from the source signals;
3) The incoming signals are numbered 1 to K, and the signal numbers are known.

3. PROPOSED

The ULA is divided into two overlapping sub-arrays. The first sub-array comprises the first $2L$ sensors, while the other sub-array comprises the last $2L$ sensors. The outputs of the two sub-arrays can be given by

$$\begin{aligned} \mathbf{Z}_1(t) &= [z_{-L}(t), \ldots, z_0(t), \ldots, z_{L-1}(t)]^T \\ \mathbf{Z}_2(t) &= [z_{-L+1}(t), \ldots, z_0(t), \ldots, z_L(t)]^T \end{aligned} \tag{5}$$

It is obvious that the common characteristic of near-field and far-field sources is α_k, and the differences consist in that β_k is approximately equal to zero for far-field sources but nonzero for near-field sources,

which means that we can construct some cumulant matrices that contain the common term α_k no matter whether these sources are near-field sources or far-field sources. In this way, α_k exists in both far-field and near-field sources, which can be estimated by the conventional high-resolution algorithms.

High-order cumulant technique can increase both the estimation accuracy and the degree of freedom for an array with given sensor number [17, 18]. In addition, higher than third order cumulant of Gaussian random process would be equal to zero [19]. Motivated by these properties, fourth-order cumulant is chosen as a key technique in this paper.

Firstly, the proposed algorithm begins with the fourth-order cumulant of the array outputs. The symmetry definition of fourth-order cumulant of the zero-mean stationary random process can be given as follows:

$$\begin{aligned}
&\mathrm{cum}(z_i(t), z_p(t), z_q^*(t), z_j^*(t)) \\
&= \mathrm{cum}\left(\sum_{k=1}^{K} e^{j(\alpha_k i+\beta_k i^2)} s_k(t), \sum_{k=1}^{K} e^{j(\alpha_k p+\beta_k p^2)} s_k(t), \sum_{k=1}^{K} e^{-j(\alpha_k q+\beta_k q^2)} s_k^*(t), \sum_{k=1}^{K} e^{-j(\alpha_k j+\beta_k j^2)} s_k^*(t)\right) \\
&\quad +\mathrm{cum}(n_i(t), n_p(t), n_q^*(t), n_j^*(t)) \\
&= \sum_{k=1}^{K} e^{j\alpha_k[(i-q)-(j-p)]+j\beta_k[(i^2-q^2)-(j^2-p^2)]}\gamma_k \\
&\quad i, j, p, q \in \{-L, -L+1, \ldots, L\}
\end{aligned} \tag{6}$$

where $\gamma_k = \mathrm{cum}(s_k(t),\, s_k(t),\, s_k^*(t),\, s_k^*\,(t))$ is the kurtosis of the k-th signal, and i, j, p, q are the indexes of sensors. It is noticed that both $i - q \neq j - p$ and $i^2 - q^2 = j^2 - p^2$ are required to retain the α_k and remove the β_k. For this purpose, the parameters should be set as $q = -i$ and $p = -j$. Thus, Eq. (6) becomes

$$\mathrm{cum}(z_i(t), z_{-j}(t), z_{-i}^*(t), z_j^*(t)) = \sum_{k=1}^{K} e^{j\alpha_k 2(i-j)}\gamma_k \quad i, j \in \{-L, -L+1, \ldots, L\} \tag{7}$$

Based on the above observation, a special fourth-order cumulant matrix $\mathbf{C}_1 \in C^{2L\times 2L}$ which only contains the data received by sub-array 1 can be defined as

$$\begin{aligned}
\mathbf{C}_1(L+1+i, L+1+j) &= \mathrm{cum}\left(z_i(t), z_{-1-j}(t), z_{-1-i}^*(t), z_j^*(t)\right) = \sum_{k=1}^{K} e^{j(\alpha_k-\beta_k)[(2i+1)-(2j+1)]}\gamma_k \\
&\quad i, j \in \{-L, -L+1, \ldots, L-1\}.
\end{aligned} \tag{8}$$

Similarly, another special fourth-order cumulant matrix $\mathbf{C}_2$ of sub-array 2 can be given by

$$\begin{aligned}
\mathbf{C}_2(L+i, L+j) &= \mathrm{cum}\left(z_i(t), z_{1-j}(t), z_{1-i}^*(t), z_j^*(t)\right) = \sum_{k=1}^{K} e^{j(\alpha_k+\beta_k)[(2i-1)-(2j-1)]}\gamma_k \\
&\quad i, j \in \{-L+1, -L+2, \ldots, L\}
\end{aligned} \tag{9}$$

To construct a Hermite matrix, a cross correlation matrix of sub-array 1 and sub-array 2 is needed, which is defined as matrix $\mathbf{C}_3$. The matrix $\mathbf{C}_3$ is actually the cross fourth-order cumulant matrix of sub-array 1 and sub-array 2.

$$\begin{aligned}
\mathbf{C}_3(L+1+i, L+j) &= \mathrm{cum}\left(z_i(t), z_{1-j}(t), z_{-1-i}^*(t), z_j^*(t)\right) = \sum_{k=1}^{K} e^{j(\alpha_k-\beta_k)(2i+1)} e^{-j(\alpha_k+\beta_k)(2j-1)}\gamma_k \\
&\quad i \in \{-L, -L+1, \ldots, L-1\}, \quad j \in \{-L+1, -L+2, \ldots, L\}
\end{aligned} \tag{10}$$

Then, collecting the three matrices $\mathbf{C}_1$, $\mathbf{C}_2$, and $\mathbf{C}_3$, a $4L \times 4L$ Hermite matrix is described as

$$\mathbf{C} = \begin{bmatrix} \mathbf{C}_1 & \mathbf{C}_3^H \\ \mathbf{C}_3 & \mathbf{C}_2 \end{bmatrix} \tag{11}$$

Note that the matrix $\mathbf{C}$ can be expressed in a compact matrix form

$$\mathbf{C} = \mathbf{B}\mathbf{C}_\gamma\mathbf{B}^H \tag{12}$$

where $\mathbf{C}_\gamma = \text{diag}[\gamma_1, \gamma_2, \ldots, \gamma_K]$, and $\mathbf{B}$ is the steering matrix. According to the way of array partition, matrix $\mathbf{B}$ can be divided into two parts

$$\mathbf{B} = \begin{bmatrix} \mathbf{B}_1 \\ \mathbf{B}_2 \end{bmatrix} \tag{13}$$

where $\mathbf{B}_1$, $\mathbf{B}_2 \in C^{2L\times K}$ are the steering matrixes of sub-array 1 and sub-array 2, which is given by

$$\begin{aligned}
\mathbf{B}_17 &= \begin{bmatrix} e^{j(\alpha_1-\beta_1)(-2L+1)} & e^{j(\alpha_2-\beta_2)(-2L+1)} & \cdots & e^{j(\alpha_K-\beta_K)(-2L+1)} \\ e^{j(\alpha_1-\beta_1)(-2L+3)} & e^{j(\alpha_2-\beta_2)(-2L+3)} & \cdots & e^{j(\alpha_K-\beta_K)(-2L+3)} \\ \vdots & \vdots & \ddots & \vdots \\ e^{j(\alpha_1-\beta_1)(2L-1)} & e^{j(\alpha_2-\beta_2)(2L-1)} & \cdots & e^{j(\alpha_K-\beta_K)(2L-1)} \end{bmatrix} \\
\mathbf{B}_2 &= \begin{bmatrix} e^{j(\alpha_1+\beta_1)(-2L-1)} & e^{j(\alpha_2+\beta_2)(-2L-1)} & \cdots & e^{j(\alpha_K+\beta_K)(-2L-1)} \\ e^{j(\alpha_1+\beta_1)(-2L+1)} & e^{j(\alpha_2+\beta_2)(-2L+1)} & \cdots & e^{j(\alpha_K+\beta_K)(-2L+1)} \\ \vdots & \vdots & \ddots & \vdots \\ e^{j(\alpha_1+\beta_1)(2L+1)} & e^{j(\alpha_2+\beta_2)(2L+1)} & \cdots & e^{j(\alpha_K+\beta_K)(2L+1)} \end{bmatrix}
\end{aligned} \tag{14}$$

To estimate the AOAs of mixed near-field and far-field sources, the singular decomposition of$\mathbf{C}$ should be implemented by

$$\mathbf{C} = \mathbf{V}\mathbf{\Sigma}\mathbf{V}^H = \sum_{k=1}^{K} \mu_k v_k v_k^H \tag{15}$$

where $\Sigma \in C^{K\times K}$ is a diagonal matrix which contains nonzero eigenvalues; $\mathbf{V}\in C^{4L\times K}$ is the matrix of eigenvectors; μ_k is nonzero eigenvalue; v_k is its corresponding eigenvector. Hence $\mathbf{V}_s = [v_1, v_2, \ldots, v_k]$ spans the signal subspace of $\mathbf{C}$.

Similarly, $\mathbf{V}_s$ can also be divided into two vectors $\mathbf{V}_1$, $\mathbf{V}_2 \in C^{2L\times K}$

$$\mathbf{V}_s = \begin{bmatrix} \mathbf{V}_1 \\ \mathbf{V}_2 \end{bmatrix} \tag{16}$$

It is obvious that $\mathbf{V}_s$ and $\mathbf{B}$ span the same signal subspace, and then the spatial linear transformation can be described in following form as

$$\mathbf{V}_s = \begin{bmatrix} \mathbf{V}_1 \\ \mathbf{V}_2 \end{bmatrix} = \mathbf{B}\mathbf{T} = \begin{bmatrix} \mathbf{B}_1\mathbf{T} \\ \mathbf{B}_2\mathbf{T} \end{bmatrix} \tag{17}$$

where $\mathbf{T}$ is a $K \times K$ full rank transformation matrix. It is noticed that $\mathbf{B}_1$ and $\mathbf{B}_2$ are vandermonde matrices. In order to avoid the spatial spectrum search and improve the estimation accuracy, we divide $\mathbf{V}_1$, $\mathbf{V}_2$, $\mathbf{B}_1$ and $\mathbf{B}_2$ as

$$\begin{aligned}
\mathbf{V}_1 &= \begin{bmatrix} \mathbf{V}_{1,F} \\ last\,row \end{bmatrix} = \begin{bmatrix} first\,row \\ \mathbf{V}_{1,B} \end{bmatrix} \\
\mathbf{V}_2 &= \begin{bmatrix} \mathbf{V}_{2,F} \\ last\,row \end{bmatrix} = \begin{bmatrix} first\,row \\ \mathbf{V}_{2,B} \end{bmatrix} \\
\mathbf{B}_1 &= \begin{bmatrix} \mathbf{B}_{1,F} \\ last\,row \end{bmatrix} = \begin{bmatrix} first\,row \\ \mathbf{B}_{1,B} \end{bmatrix} \\
\mathbf{B}_2 &= \begin{bmatrix} \mathbf{B}_{2,F} \\ last\,row \end{bmatrix} = \begin{bmatrix} first\,row \\ \mathbf{B}_{2,B} \end{bmatrix}
\end{aligned} \tag{18}$$

According to Eq. (17), the following equations hold

$$\begin{aligned}
\mathbf{V}_{1,F} &= \mathbf{B}_{1,F}\mathbf{T} \\
\mathbf{V}_{1,B} &= \mathbf{B}_{1,F}\mathbf{\Phi}_1\mathbf{T} \\
\mathbf{V}_{2,F} &= \mathbf{B}_{2,F}\mathbf{T} \\
\mathbf{V}_{2,B} &= \mathbf{B}_{2,F}\mathbf{\Phi}_2\mathbf{T}
\end{aligned} \tag{19}$$

where $\Phi_{-d/2}$ and $\Phi_{d/2}$ are $K \times K$ diagonal matrixes

$$\begin{aligned} \mathbf{\Phi}_1 &= \text{diag}\left[e^{j2(\alpha_1-\beta_1)}, e^{j2(\alpha_2-\beta_2)}, \ldots, e^{j2(\alpha_K-\beta_K)}\right] \\ \mathbf{\Phi}_2 &= \text{diag}\left[e^{j2(\alpha_1+\beta_1)}, e^{j2(\alpha_2+\beta_2)}, \ldots, e^{j2(\alpha_K+\beta_K)}\right] \end{aligned} \tag{20}$$

Then, Eq. (19) can be expressed as

$$\begin{aligned} \mathbf{V}_{1,B} &= \mathbf{V}_{1,F}\mathbf{T}^{-1}\mathbf{\Phi}_1\mathbf{T} = \mathbf{V}_{1,F}\mathbf{\Psi}_1 \\ \mathbf{V}_{2,B} &= \mathbf{V}_{2,F}\mathbf{T}^{-1}\mathbf{\Phi}_2\mathbf{T} = \mathbf{V}_{2,F}\mathbf{\Psi}_2 \end{aligned} \tag{21}$$

Based on the fact that $\mathbf{V}_1$ and $\mathbf{V}_2$ are column full rank matrices, and two transformation matrices Ψ_1, $\Psi_2 \in C^{K\times K}$ can be expressed as

$$\begin{aligned} \mathbf{\Psi}_1 &= \left(\mathbf{V}_{1,F}^H\mathbf{V}_{1,F}\right)^{-1}\mathbf{V}_{1,F}^H\mathbf{V}_{1,B} \\ \mathbf{\Psi}_2 &= \left(\mathbf{V}_{2,F}^H\mathbf{V}_{2,F}\right)^{-1}\mathbf{V}_{2,F}^H\mathbf{V}_{2,B} \end{aligned} \tag{22}$$

The singular decomposition of Ψ_1 and Ψ_2 should be implemented by

$$\begin{aligned} \mathbf{\Psi}_1 &= \mathbf{T}^H\mathbf{\Phi}_1\mathbf{T} \\ \mathbf{\Psi}_2 &= \mathbf{T}^H\mathbf{\Phi}_2\mathbf{T} \end{aligned} \tag{23}$$

Thus, α_k and β_k can be estimated by singular decomposition of Ψ_1 and Ψ_2 [20].

It must be noticed that when the k-th source is FF source, $\Phi_1(k,k) = \Phi_2(k,k)$, but not for near field source. Thus, this method can classify rapidly whether the k-th source is a NF source or FF source.

It is undeniable that the algebraic expression such as Eq. (24) can be used to estimate θ_k

$$\hat{\theta}_k = \arcsin\left(\frac{\arg\left[\mathbf{\Phi}_1(k,k)\mathbf{\Phi}_2(k,k)\right]}{-8\pi d/\lambda}\right) \tag{24}$$

After estimating the AOAs of all sources, it is obvious that the range parameter of NF sources can be calculated by

$$\hat{r}_k = \frac{4\pi d^2\cos\left(\hat{\theta}_k\right)/\lambda}{\arg\left[\mathbf{\Phi}_2(k,k)/\mathbf{\Phi}_1(k,k)\right]} \tag{25}$$

4. DISCUSSION

4.1. Number of Array Elements and Sources

Based on the subspace theory, at least one eigenvector from eigendescomposition of constructed matrix is needed to be reserved for spanning the noise subspace. Therefore, the number of processed sources must be less than the minimal value between the number of rows and that of columns. Note that the array is divided into two sub-arrays with $2L$ elements, and the dimension of fourth-order cumulant matrix $\mathbf{C}_1$ and $\mathbf{C}_2$ is $2L$. Therefore, the proposed algorithm can localize $2L-1$ sources at most by using a ULA with $2L+1$ elements.

4.2. Estimation Accuracy

Based on the fourth-order cumulant algorithm, the kurtosis of Gaussian noise is 0. Therefore, the estimation accuracy will increase as the influence of noise decreases.

4.3. Computational Complexity

Major computational loads involve cumulant matrix construction, eigendecomposition implementation, ESPRIT algorithm. It is defined that the search step of DOA $\theta \in [-\pi/2, \pi/2]$ is $\Delta\theta$, and the search step of $r \in [0.62(D^3/\lambda)^{1/2}, 2D^2/\lambda]$ is Δr for K_1 far-field sources. For Cum4MUSIC, the major computations

are forming two $(2L+1)\times(2L+1)$ matrices, and to eigenvalue decompose the two matrix for spatial searching. Thus, the computational complexity of Cum4MUSIC algorithm is

$$2(2L+1)^2M+\frac{8}{3}(2L+1)^3+2\frac{\pi}{\Delta\theta}(2L+1)^2+(K-K_1)\frac{2D^2/\lambda-0.62(D^3/\lambda)^{1/2}}{\Delta r}(2L+1)^2$$

where M is the number of snapshots.

The major computational complexity of the proposed algorithm is to form three $2L\times 2L$ fourth-order cumulant matrices, and eigendecompose a $4L\times 4L$ matrix. Then, we use the ESPRITE algorithm to estimate the DOAs with eigendecomposing two $(2L-1)\times(2L-1)$ matrices. Thus, the computational complexity of proposed algorithm is

$$3(2L)^2M+\frac{4}{3}(4L)^3+\frac{8}{3}(2L-1)^3$$

Therefore, it can be clearly seen that the proposed algorithm has lower computational cost.

4.4. Capacity for Localizing Mixed Near-Field and Far-Field Sources

From the above analysis, we can see that if the far-field source and near-field source have the same DOA at the center of the array, the conventional MUSIC-like algorithm would be invalid. However, using the proposed algorithm, the DOAs of each source at different phase reference points can be worked out, and the FF and NF can be classified efficiently [21–23].

5. SIMULATION RESULT

Some simulation results are presented to evaluate the performance of the proposed algorithm. A ULA of 7-elements with inter-element spacing $d=\lambda/4$ is taken into consideration. The input signal to noise ratio (SNR) of the k-th source is defined as $10\times\log_{10}(\sigma_k^2/\sigma_n^2)$, where σ_k^2 denotes the power of the k-th source, and σ_n^2 denotes the noise power. Assume that all sources are with equal power and that the number of sources is known as *a prior*. For comparison, the Cum4MUSIC and TSMUSIC would be executed. The results shown following are evaluated by the estimated root mean square error (RMSE) from the average results of 100 independent Monte Carlo experiments.

It is noticed that the estimation performance of the range parameters are only for near-field sources experiment, and we would not give the estimation performance of the range parameters of far-field sources. Because we believe that the range of far-field sources is infinite.

5.1. Mixed Far-Field and Near-Field Sources

We consider a scenario that one FF and one NF sources coexist, and the locations parameters are $f\theta_1=-10^\circ$, $r_1=+\infty g$ and $f\theta_2=20^\circ$, $r_2=2\lambda g$. The snapshot number is set as 1024, and the signal-to-noise ratio (SNR) varies from -5 dB to 20 dB.

Under the given experimental conditions, the DOA estimation and range estimation spectrum is shown by simulation.

Figure 1 shows the DOA spectra of TSMUSIC. It is clear that the algorithm needs spectra searching twice, i.e., the FF and NF sources are estimated separately. After DOA estimating, the range is calculated in algebraic way. Fig. 2 shows the DOA spectra of Cum4MUSIC, which shows that the FF and NF sources are estimated by spectra searching once. After that, the range of NF source is searched with estimated DOA of NF source as shown in Fig. 3.

From Fig. 4 and Fig. 5, it is shown that for both the FF and NF sources, the AOA performance of proposed method is close to TSMUSIC and much better than Cum4MUSIC. However, the proposed algorithm achieves the best DOA estimation performance for both far-field and near-field sources among the three algorithms.

From Fig. 6, we can see that the proposed algorithm achieves better estimation accuracy of range parameters than both TSMUSIC and Cum4MUSIC algorithms. This is because: 1) to estimate the range parameters, the proposed algorithm is based on the higher accuracy AOA estimates than both the TSMUSIC and Cum4MUSIC algorithms; 2) especially, the proposed algorithm avoids any spectral searching which would yield additional error.

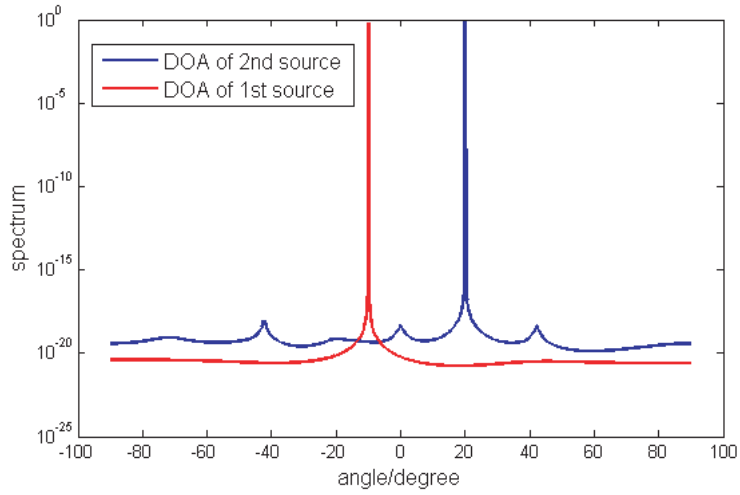

Figure 1. The DOA spectra of TSMUSIC.

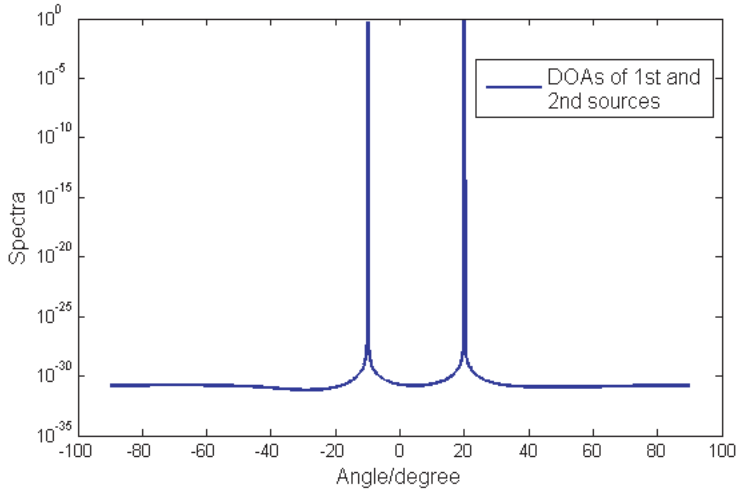

Figure 2. The DOA spectra of Cum4MUSIC.

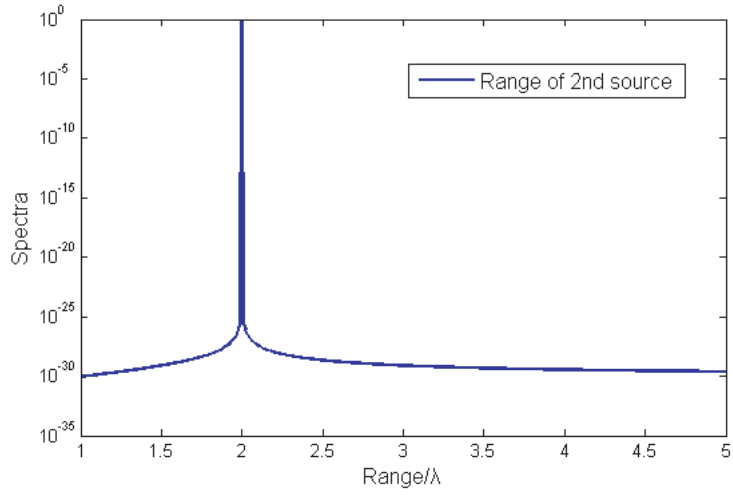

Figure 3. The range spectra of Cum4MUSIC.

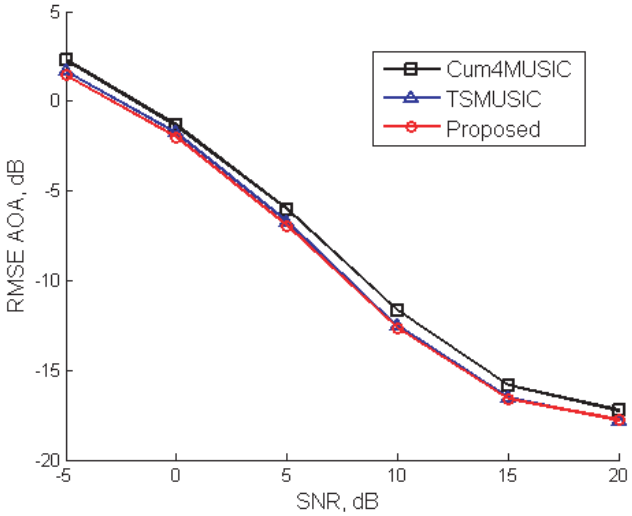

Figure 4. RMSEs of 1-th source AOA estimation versus SNR.

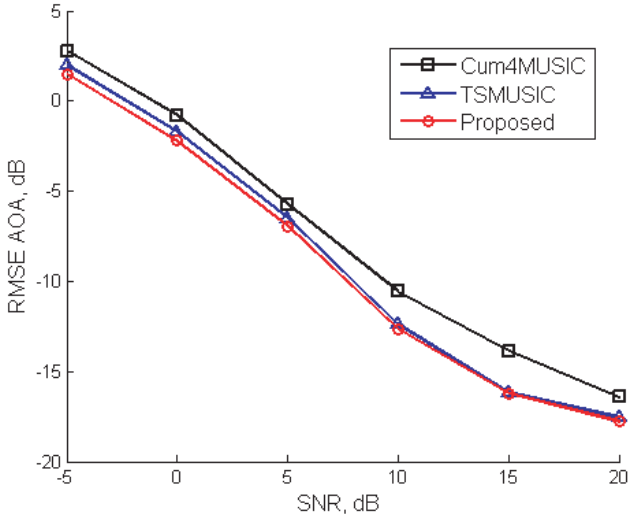

Figure 5. RMSEs of 2-th source AOA estimation versus SNR.

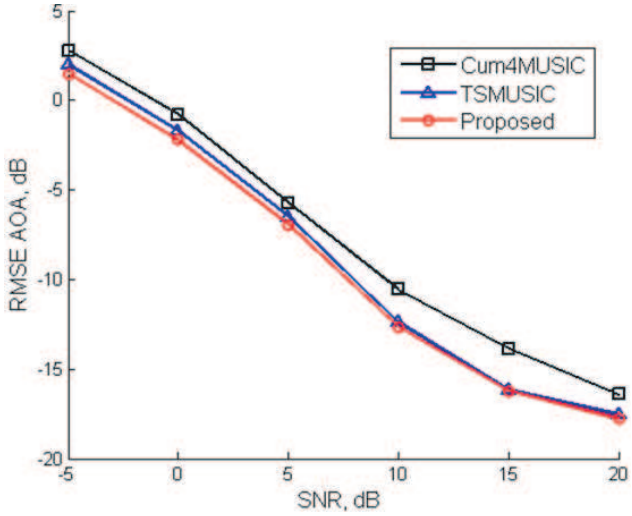

Figure 6. RMSEs of 2-th source range estimation versus SNR.

5.2. Pure Near-Field Sources

We consider the case with only two near-field sources which are located at $f\theta_3 = -10°$, $r_1 = 1.5\lambda g$ and $f\theta_4 = -10°$, $r_2 = 2.6\lambda g$. It can be seen that the two sources have the same AOA. The snapshot number is set as 1024, and the signal-to-noise ratio (SNR) varies from -5 dB to 20 dB.

Under the given experimental conditions, the DOA estimation and range estimation spectrum are shown by simulation.

Figure 7 shows the DOA spectra of TSMUSIC, which contains the spectra of NF sources only. Fig. 8 shows the DOA spectra of Cum4MUSIC. It shows that the DOAs of two NF sources are estimated by spectra searching once. After that, the ranges of two NF source are estimated as shown in Fig. 9.

In combination of Figs. 1–3 and Figs. 7–9, it is clear that TSMUSIC can classify the FF and NF sources, but Cum4MUSIC must need all the sources as prior knowledge.

From Fig. 10, Fig. 11 and Fig. 12, it can be observed that for pure near-field sources scenario, the proposed algorithm still outperforms TSMUSIC and Cum4MUSIC for both AOA and range estimation. Besides, the RMSEs of both AOA and range estimates decrease monotonically as the SNR increases.

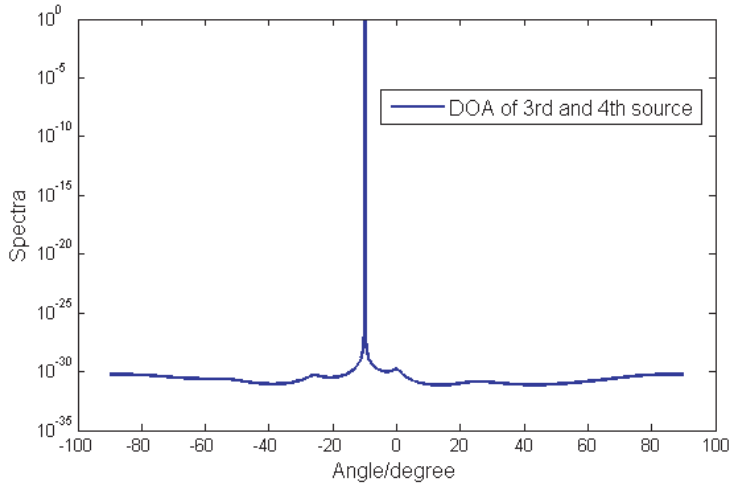

Figure 7. The range spectra of TSMUSIC.

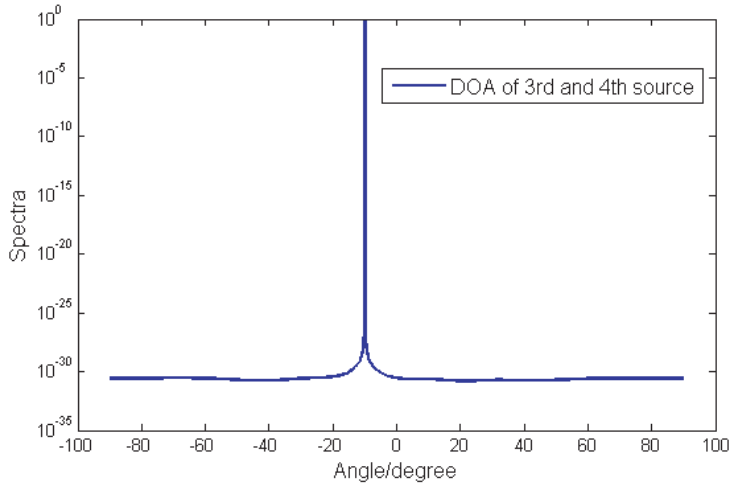

Figure 8. The DOA spectra of Cum4MUSIC.

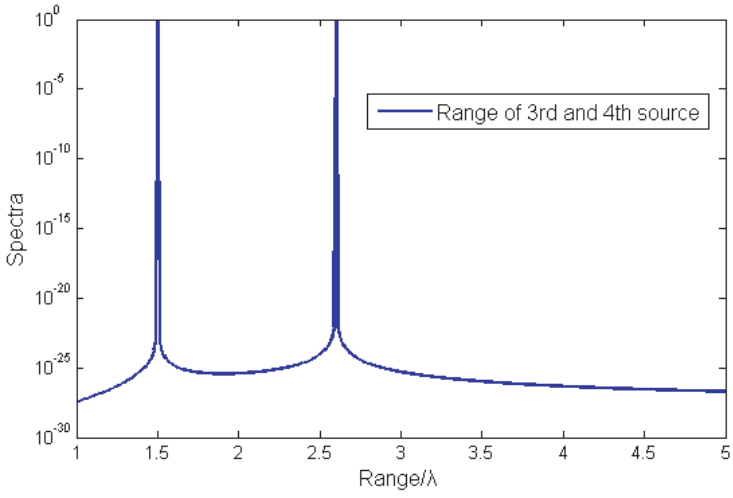

Figure 9. The range spectra of Cum4MUSIC.

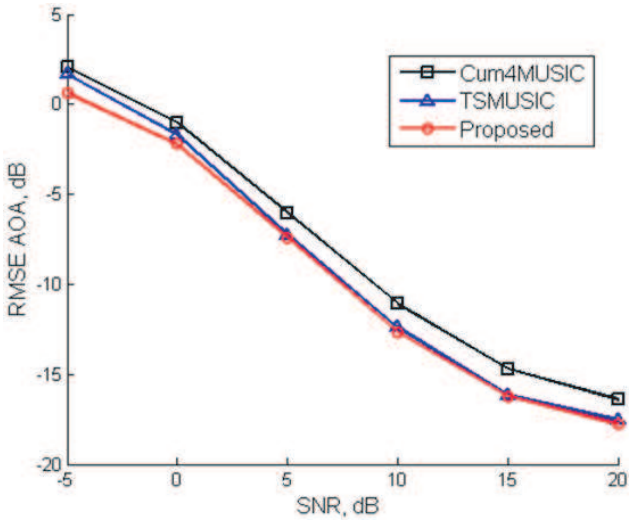

Figure 10. RMSEs of 3-rd and 4-th sources AOA estimation versus SNR.

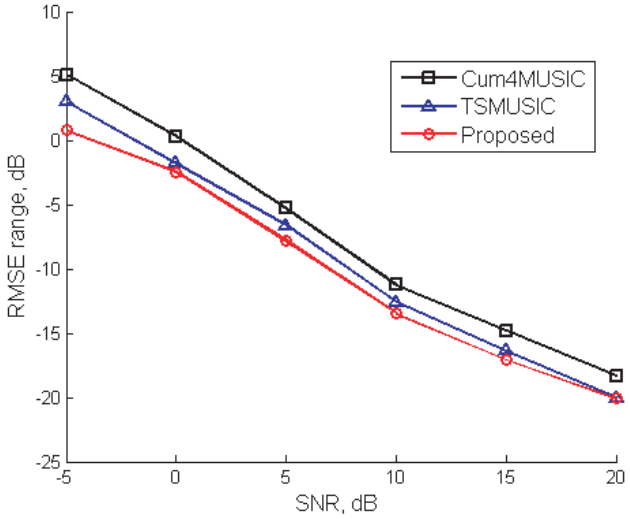

Figure 11. RMSEs of 3-rd source range estimation versus SNR.

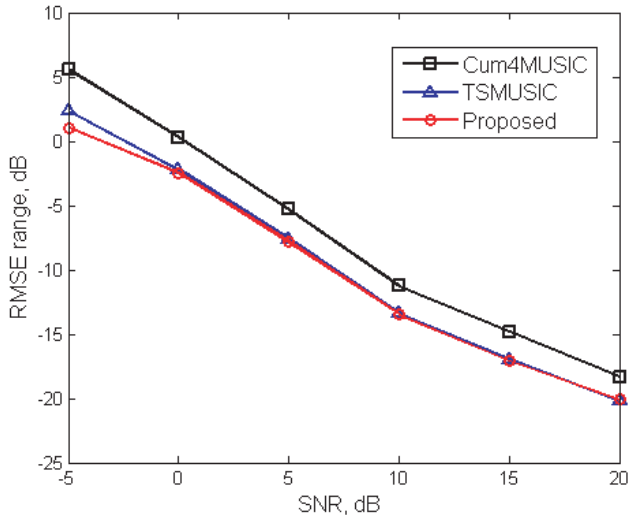

Figure 12. RMSEs of 4-th source range estimation versus SNR.

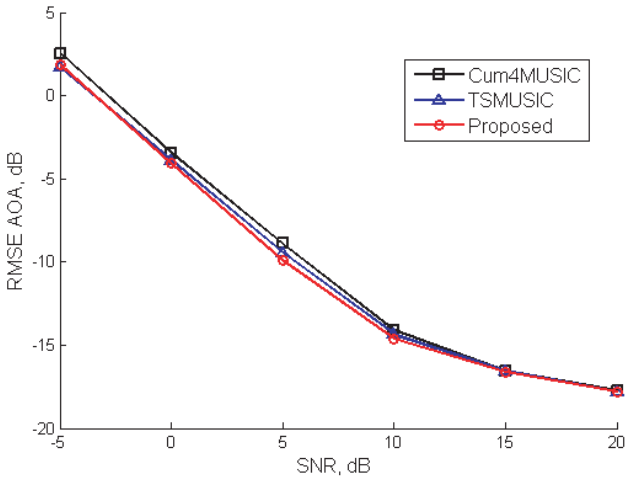

Figure 13. RMSEs of 5-th source range estimation versus SNR.

The DOA and range parameters of the proposed algorithm are estimated without spatial spectrum searching, so that it is inconvenient to give DOA and range spectrums for the proposed algorithm.

5.3. Pure Far-Field Sources

In the last experiment, only two far-field sources are considered, and the locations parameters are $f\theta_5 = -40^{circ}$, $r_1 = +\infty g$ and $f\theta_6 = 20°$, $r_2 = +\infty g$. The snapshot number is set as 1024, and the signal-to-noise ratio (SNR) varies from -5 dB to 20 dB.

From Fig. 13 and Fig. 14, we can see that in the case of pure far-field sources, the estimation accuracies of TSMUSIC and Cum4MUSIC are close to each other, while the proposed algorithm has the best performance. Besides, the RMSEs of DOA estimations for these three algorithms decrease as the SNR increases, which approaches the CRLB.

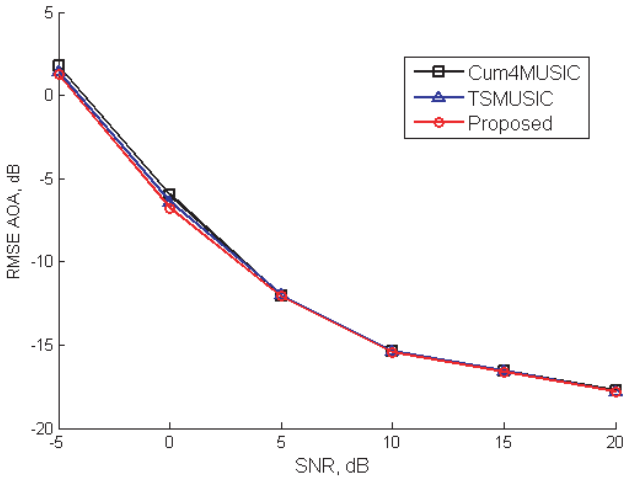

Figure 14. RMSEs of 6-th source range estimation versus SNR.

6. CONCLUSION

Based on constructing a special fourth-order cumulant matrix and regrouping the source subspace, two transformation matrices which contain the AOAs and ranges of all sources can be obtained. According to aforementioned formulas, the two transformation matrices are constructed by first-order and second-order terms in two different ways. Thus, the AOAs of both FF and NF sources can be calculated without spectral search which implies a very high computational cost, as well as the range of NF sources. Meanwhile, we can rapidly classify whether any source is NF source or FF source. Compared with TSMUSIC and Cum4MUSIC algorithm, the proposed method is effective in sources location with low computational cost, and rapid in sources classification.

ACKNOWLEDGMENT

This work was supported by the National Natural Science Foundation of China (Nos. 61301093, 61601372, and 61601373).

REFERENCES

1. Li, S., W. Liu, D. Zheng, S. Hu, and W. He, "Localization of near-field sources based on sparse signal reconstruction with regularization parameter selection," *International Journal of Antennas and Propagation*, Vol. 2017, Article ID 1260601, 7 pages, 2017.
2. Qin, S., Y. D. Zhang, Q. Wu, and M. G. Amin, "Structure-aware Bayesian compressive sensing for near-field source localization based on sensor-angle distributions," *International Journal of Antennas and Propagation*, Vol. 2015, Article ID 783467, 15 pages, 2015.
3. Schmidt, R. O., "Multiple emitter location and signal parameter estimation," *IEEE Trans. Antennas Propag.*, Vol. 34, 276–280, Mar. 1986.
4. Weiss, A. J. and B. Friedlander, "Range and bearing estimation using polynomial rooting," *IEEE J. Ocean. Eng.*, Vol. 18, No. 2, 130–137, Apr. 1993.
5. Roy, R. and T. Kailath, "ESPRIT-estimation of signal parameters via rotational invariance techniques," *IEEE Trans. Acoust., Speech, Signal Process.*, Vol. 37, 984–995, Jul. 1989.
6. Xie, J., H. Tao, X. Rao, and J. Su, "Localization of mixed far-field and near-field sources under unknown mutual coupling," *IEEE Trans. Digital Signal Processing*, Vol. 50, No. 3, 229–239, 2016.

7. Xie, J., H. Tao, X. Rao, and J. Su, "Passive localization of mixed far-field and near-field sources without estimating the number of sources," *IEEE Trans. Sensors*, Vol. 15, No. 2, 3834–3853, 2015.
8. Liang, J. and D. Liu, "Passive localization of mixed near-field and far-field sources using two-stage MUSIC algorithm," *IEEE Trans. Signal Processing*, Vol. 58, 108–120, 2010.
9. Grosicki, E., K. Abed-Meraim, and Y. Hua, "A weighed linear prediction method for near-field source localization," *IEEE Trans. Signal Processing*, Vol. 53, 3651–3660, Oct. 2005.
10. Liu, G. and X. Sun, "Two-stage matrix differencing algorithm for mixed far-field and near-field sources classification and localization," *Sens. J.*, Vol. 14, 1957–1965, 2014.
11. Wu, Y. T., H. Wang, Y. B. Zhang, and Y. Wang, "Multiple near-field source localisation with uniform circular array," *IEEE Electron. Lett.*, Vol. 49, No. 24, 1509–1510, 2013.
12. Xue, B., G. Y. Fang, and Y. C. Ji, "Passive localisation of mixed far-field and near-field sources using uniform circular array," *IEEE Electron. Lett.*, Vol. 52, No. 20, 1690–1692, 2016.
13. Xie, J., H. H. Tao, X. Rao, and J. Su, "Localization of mixed far-field and near-field sources under unknown mutual coupling," *IEEE Trans. Digital Signal Processing*, Vol. 50, No. 3, 229–239, 2016.
14. Yuen, N. and B. Friedlander, "Performance analysis of higher order ESPRIT for localization of near-field sources," *IEEE Trans. Signal Processing*, Vol. 46, 709–719, Aug. 1998.
15. Challa, R. N. and S. Shamsunder, "High-order subspace based algorithms for passive localization of near-field sources," *Proc. 29th Asilomar Conf. Signals, Syst. Comput.*, Vol. 2, 777–781, Oct. 1995.
16. Zhang, Y. D., Q. Siam and M. G. Amin, "Near-field source localization based on sparse reconstruction of sensor-angle distributions," *IEEE International Conference on Radar Conference*, 891–895, May 2015.
17. Dogan, M. C. and J. M. Mendel, "Applications of cumulants to array processing — Part I: Aperture extension and array calibration," *IEEE Trans. Signal Processing*, Vol. 43, 1200–1216, May 1995.
18. Porat, B. and B. Friedlander, "Direction finding algorithms based on high-order statistics," *IEEE Trans. Signal Processing*, Vol. 39, 2016–2024, Sep. 1999.
19. Chevalier, P. and A. Ferreol, "On the virtual array concept for the fourth-order direction finding problem," *IEEE Trans. Signal Processing*, Vol. 47, 2592–2595, May 1999.
20. Roy, R. and T. Kailath, "ESPRIT-estimation of signal parameters via rotational invariance techniques," *IEEE Trans. ASSP*, Vol. 37, 984–995, Jul. 1989.
21. Yildirim, A., A. Gokdogan, and M. Merdan, "Numerical approximations to the solution of ray tracing through the crystalline lens," *Chinese Physics Letters*, Vol. 29, No. 7, Article Number: 074202, Jul. 2012.
22. Vazquez-Leal, H., U. Filobello-Nino, and A. Yildirim, "Transient and DC approximate expressions for diode circuits," *IEICE Electronics Express*, Vol. 9, No. 6, 522–530, Mar. 2012.
23. Yuzbasi, S., N. Sahin, and A. Yildirim, "A collocation approach for solving high-order linear Fredholm-Volterra integro-differential equations," *Mathematical and Computer Modelling*, Vol. 55, No. 3–4, 547–563, Feb. 2012.